



*Citation for published version:*

Baïri, A, Martin Garin, A, Adeyeye, K, She, K & Millán-García, JA 2020, 'Enhancement of natural convection for improvement of Trombe wall performance. An experimental study', *Energy and Buildings*, vol. 211, 109788. <https://doi.org/10.1016/j.enbuild.2020.109788>

*DOI:*

[10.1016/j.enbuild.2020.109788](https://doi.org/10.1016/j.enbuild.2020.109788)

*Publication date:*

2020

*Document Version*

Peer reviewed version

[Link to publication](#)

*Publisher Rights*

CC BY-NC-ND

## University of Bath

### Alternative formats

If you require this document in an alternative format, please contact:  
[openaccess@bath.ac.uk](mailto:openaccess@bath.ac.uk)

**General rights**

Copyright and moral rights for the publications made accessible in the public portal are retained by the authors and/or other copyright owners and it is a condition of accessing publications that users recognise and abide by the legal requirements associated with these rights.

**Take down policy**

If you believe that this document breaches copyright please contact us providing details, and we will remove access to the work immediately and investigate your claim.

# Enhancement of natural convection for improvement of Trombe wall performance. An experimental study.

A. Baïri<sup>1,\*</sup>, A. Martín-Garín<sup>2</sup>, K. Adeyeye<sup>3</sup>, K. She<sup>4</sup>, J.A. Millán-García<sup>2</sup>

<sup>1</sup> Université de Paris, Laboratoire Thermique Interfaces Environnement (LTIE), EA 4415, Département GTE, 50, Rue de Sèvres, F-92410 Ville d'Avray, France

<sup>2</sup> University of the Basque Country UPV/EHU, ENEDI Research Group, Department of Thermal Engineering, Plaza Europa 1, 20018 Donostia-San Sebastián, Spain

<sup>3</sup> University of Bath, Department of Architecture and Civil Engineering, Claverton Down, Bath BA2 7AY, UK <sup>4</sup> University of Brighton, Lewes Road, Brighton, BN1 5EL, UK

<sup>4</sup> University of Brighton, School of Environment and Technology, SET, Brighton, UK

## Abstract

This experimental work shows that the natural convective heat transfer in the active enclosure of a conventional Trombe wall assembly is enhanced by the interposition of transparent and vertical partitions. Quantification of the average Nusselt number corresponding to both versions with and without partitions was carried out by means of a 1/5 scale assembly. The glass cover is maintained isothermal at cold temperature while the active wall generates a variable heat flux simulating the incident solar radiation. The distance between the two active and parallel walls is variable. Four ratios between this distance and the height of the wall are considered, associated with a wide range of Rayleigh number reaching  $4.1 \times 10^9$ . An error calculation is carried out for all the processed configurations, taking into account the experimental uncertainties of the measured physical parameters. The maximum error found on the average Nusselt number is low, of about 5%. Measurements made by means of an interstitial medium without partitions are consistent with the results of other work carried out by experimental and numerical approaches in specific ranges of Rayleigh number. This study reveals the partitions effectiveness, since the natural convective heat transfer's increase lies between 10.0% and 14.4% according to the considered configuration. Correlations are proposed in the present work in order to calculate the average natural convective Nusselt number for the conventional Trombe wall without partitions and for its improved version, for any aspect ratio and in the whole range of the considered Rayleigh number. They contribute to the optimization of the thermal design of this interesting assembly.

## Keywords

Natural convection, Trombe wall, Architecture, Performance enhancement, High Rayleigh number, Experimental heat transfer, Thermal measurements,

## Nomenclature

$A$	aspect ratio $A=L/H$ (-)
$a$	thermal diffusivity ( $\text{m}^2\text{s}^{-1}$ )
$E$	thickness (m)
$g$	gravity acceleration ( $\text{m}\cdot\text{s}^{-2}$ )
$h$	local convective heat transfer coefficient ( $\text{Wm}^{-2}\text{K}^{-1}$ )
$\bar{h}$	average convective heat transfer coefficient ( $\text{Wm}^{-2}\text{K}^{-1}$ )

---

\* Corresponding author Prof. A. Baïri, [abairi@u-paris10.fr](mailto:abairi@u-paris10.fr), [bairi.a@gmail.com](mailto:bairi.a@gmail.com)

$H$	height of the active cavity (m)
$I$	current intensity (A)
$L$	distance between the hot and cold walls of the active cavity (m)
$\overline{Nu}$	average Nusselt Number for the wall without partitions (-)
$\overline{Nu}_m$	average Nusselt Number for the wall equipped with partitions (-)
$P$	generated power, $P = UI$ (W)
$r^*$	improvement factor $r^* = 100(\overline{Nu}_m - \overline{Nu}) / \overline{Nu}$ (-)
$Ra$	Rayleigh number (-)
$S$	surface of the central strip of the wall (m <sup>2</sup> )
$T$	temperature (K)
$\overline{T}_h$	average surface temperature of the hot active wall (K)
$U$	voltage (V)

#### Greek symbols

$\beta$	volumetric expansion coefficient (K <sup>-1</sup> )
$\Delta m/m$	relative uncertainty corresponding to a given measured parameter $m$ (-)
$\varphi$	generated heat flux (Wm <sup>-2</sup> )
$\lambda$	thermal conductivity (Wm <sup>-1</sup> K <sup>-1</sup> )
$\mu$	dynamic viscosity (Pa.s)
$\rho$	density (kg.m <sup>-3</sup> )

#### Subscripts

a	air
c	cold
h	hot
i	thermal insulator
pc	passive cavity
v	glass
w	wall

## 1. Introduction

The architecture and thermal design of the well-known Trombe wall is a proven energy saving strategy in the building sector. A Trombe wall is a massive wall covered by an external glazing area. It is a passive heating and cooling systems exploit the solar irradiation and the ambient temperature fluctuations in order to store energy and to transmit it in the indoor space the preferable time and with the suitable rate. Other prevalent passive systems are the solar chimney, the unglazed transpired solar façade and the green walls [1]. Given the changes in global warming in recent years, the use of such simple and efficient systems, presented in [2] among others, is more relevant than ever and deserves full attention of research in this field. Several works carried out through theoretical, numerical and experimental approaches have been devoted to this assembly and various versions have been proposed to further improve its efficiency and thermal comfort. In [3], a CFD approach using the RNG k-E turbulence model has been applied to some Trombe wall configurations obtained by varying various physical parameters. Their influence on the global energy performance has been determined and lead to recommendations for optimizing the operation of the Trombe system. The work [4] concerns the renovation of buildings with this system in Istanbul (Turkey). Results show that renovation based on the Trombe wall system is much more interesting from the point of view of saving energy than changing the materials of the existing envelope. Some configurations are presented

in the review [5] where other useful information and data concerning this assembly are available. The study [6] shows that indoor temperature can be increased by the heating configuration of the Trombe wall and that the configuration efficiency is of about 10%. This interesting assembly has shown its adaptability in various parts of the world. It has been implemented among others in a subtropical location [7] as well as in Egypt [8] and Tunisia [9] where the Transient System Simulation Tool (TRNSYS) has been used to confirm the effects of the wall area on the energy performance. The aerothermal phenomena occurring in the Trombe type assembly have recently been analytically examined in [10] in order to determine the optimal conditions for thermal comfort. The study shows that these conditions can improve thermal comfort by about 38% during a typical winter week. Dimensional analysis based on the  $\pi$ -Buckingham theorem is used in [11], applied to a ventilated double façade. The many physical parameters considered in this work lead to several dimensionless numbers, allowing to determine heat transfer throughout the wall by means of some measurements, without using complex and expensive simulations.

Natural convection occurring in the active cavity of the Trombe type installation strongly depends on the incident solar radiation depending on several factors, including wall location and orientation, and time. Sun's height above the horizon, shadows worn by the objects and architecture of the building itself often lead, in the current installations, to a non-uniform distribution of solar heat flux on the hot active wall of the cavity which needs to be taken into account for a correct thermal sizing of the assembly. This aspect has been examined in previous work applied to electronics cooling. Particular configurations have been treated in [12], dealing with straight cavities whose vertical hot wall is equipped with heat sources distributed with different arrangements. The study shows the importance to consider the heat flux distribution in order to optimize the enclosure global thermal conductance. Similar work was numerically performed in [13], dealing with natural convection in a rectangular enclosure containing a liquid cooling. The flow is generated by a hot plate equipped with a 3x3 heater array. The study shows that heat transfer from the discrete heaters is not uniform while it is not influenced by the Prandtl number varying from 5 to 130. The experimental work [14] deals with the same cavity and the 3x3 heater array. The convective heat transfer is quantified for each array by means of the Nusselt number in a wide Rayleigh number range. The work [15] dealing with natural convection applied to electronic cooling by means of water-Copper nanofluid in a rectangular cavity whose hot plate generating heat flux is equipped with an array of heaters also shows that the heat transfer is different on the rows.

The energy efficiency of the Trombe wall mainly depends on the natural convective flow occurring in the upstream cavity called « active cavity » in the present work. Natural convection occurring between the glass cover and the capacitive wall depends on several physical factors. Among the most important are incident solar flux, wall orientation, thermo-optical characteristics and thickness of glass cover, wall absorption factors, internal walls emissivity, wall height, distance between hot and cold active walls, and characteristics of the materials potentially arranged in the interstice separating these active walls. Finally, it is necessary to know the natural convective transfer coefficient corresponding to the active cavity in order to correctly size the assembly from the thermal point of view. Some Nusselt-Rayleigh type correlations are available in the specialized literature dealing with natural convection, such as [16]. However, these correlations are only applicable for particular boundary conditions and it is difficult to find correlations specific to the Trombe wall and valid for all real conditions. This is what motivated the present work in which a correlation is proposed, resulting from thermal and electrical measurements on a 1/5 scale prototype with two configurations. The first one deals with a smooth wall and the second with a wall equipped with transparent and parallel partitions, arranged vertically. The distance between

active walls is variable, leading to three values of the aspect ratio of 0.1, 0.2 and 0.3, while the Rayleigh number based on the incident solar flux varies within a wide range from  $2.81 \times 10^8$  to  $4.14 \times 10^9$ . Measurement uncertainties taken into account in the error calculation lead to a Nusselt number determined with a relative uncertainty of about 5%. Correlation obtained with the least squares optimization method is associated with a high coefficient of determination. The results of this work are consistent with those of other previous studies numerically and experimentally performed in particular Rayleigh number ranges. The correlation proposed in the present work allows determination of the average number for any aspect ratio value and in whole Rayleigh number range. It contributes to the optimization of the thermal design of the Trombe wall system.

**2. The considered assembly**

The purpose of this work is to quantify through experimental measures the natural convective heat transfer concerning the active cavity of the Trombe wall type assembly when it operates in heating mode as schematized in Fig. 1.

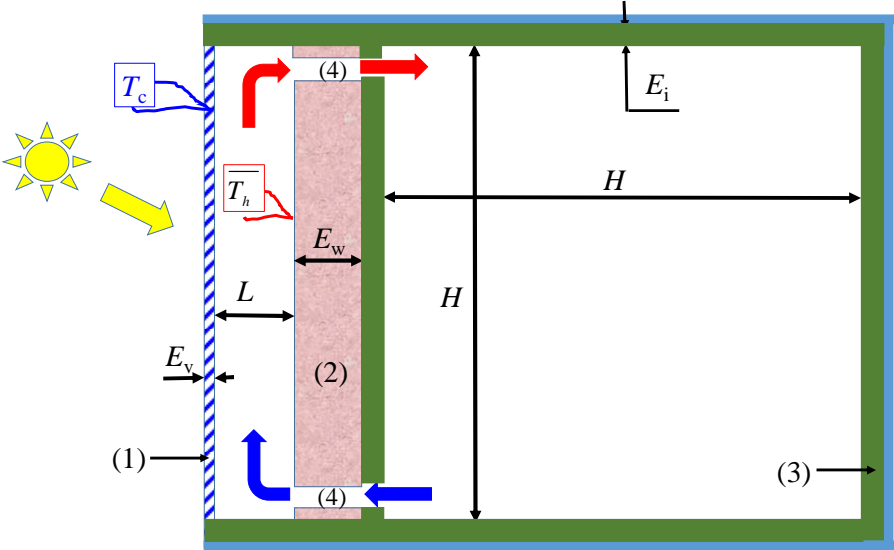


**Fig. 1.** Scheme of the considered assembly. Trombe wall operating in heating mode

The assembly tested at scale 0.2 is presented with the instrumentation used in Fig. 2a. The associated passive cavity located at the back of the wall is shown open in Fig. 2b.

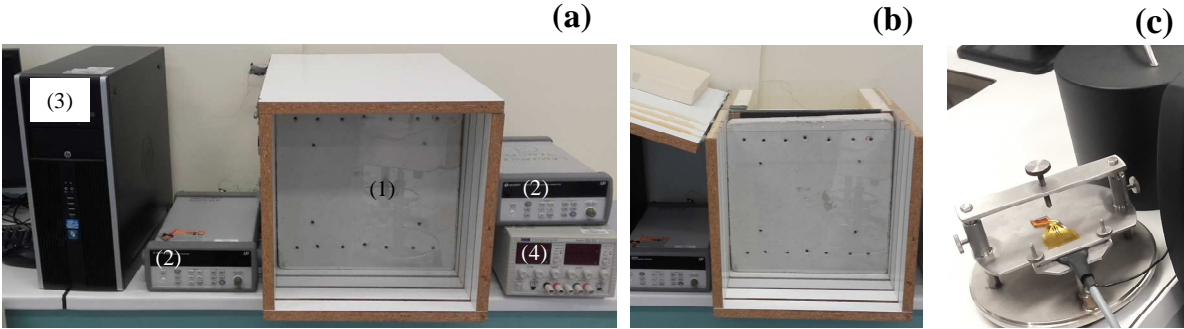


**Fig. 2.** (a) Assembly and instrumentation; (b) detail of the open passive cavity; (c) the Hot Disk TPS 2500 equipment

It consists of the four parts detailed as follows.

### 2.1. Outside glass cover

A square glass cover (1) of side  $H=550\pm 1\text{mm}$  and thickness  $E_v=3.05\pm 0.02\text{mm}$  is installed at the front of the assembly in order to produce the greenhouse effect necessary for the operation of the Trombe wall system. The spectrum of its transmission factor and its monochromatic extinction coefficient are measured by means of spectrophotometers. Its thermal conductivity has been measured by using the Hot Disk TPS 2500 equipment [17] presented in Fig. 2c based on the Transient Plane Source method [18,19]. Many measurements have been done with samples of thickness varying between 5 and  $40\pm 1\text{mm}$  arranged on one side or on both sides of probes adapted to the considered material. The measured thermal conductivity remains relatively constant in the considered temperature range ( $0-90^\circ\text{C}$ ) achieved thanks to a thermoregulated oven at  $\pm 0.5^\circ\text{C}$ . Maximum deviation is of about 4.1%. Finally, the value  $\lambda_v=0.95\pm 0.02\text{ Wm}^{-1}\text{K}^{-1}$  is adopted. The glass cover maintained isothermal at temperature  $T_c$  constitutes the cold active wall of the assembly. During the tests, this thermal condition is imposed to  $\pm 0.5^\circ\text{C}$  by installing the entire assembly in a large climatic chamber (height 2m, length 2.5m, depth 2m) whose temperature can be regulated between  $-5$  and  $+ 52^\circ\text{C} \pm 0.5^\circ\text{C}$ . This temperature-controlled climate chamber also allows assembly testing at different temperatures, and thus thermal behavior understanding according to the period of year.

### 2.2. The wall

The wall (2) in Fig 1 constitutes the active hot wall of the Trombe wall. It is made of concrete with thickness  $E_w=60\pm 1\text{mm}$  and thermal conductivity  $\lambda_w=1.42\text{ Wm}^{-1}\text{K}^{-1}$  measured with the same TPS method and accuracy as for the glass cover, using probes and a technique adapted to this material. A hot plate is inserted in the median plane of this wall. An electrical device allows generation of the desired heat flux corresponding to the incident solar flux. Vents (4) in Fig. 1 located at the bottom and top of the wall allow air entering and exiting in the active enclosure. The heating plate consists of 5 vertical strips of 3 independent electric resistances juxtaposed (Fig. 3a) and of the same surface. They are manufactured with resistive tracks of  $0.20\pm 0.03\text{ mm}$  width separated by  $0.12\pm 0.03\text{ mm}$  over a conventional single-sided Printed Circuit Board (PCB) 2mm thick epoxy with a copper layer of  $35\text{ }\mu\text{m}$  thick. The PCB equipped with thermocouples and electrical wiring is integrated in the median plane of a mold in which concrete is poured. The hot wall (Fig. 3b) is square (side  $H=550\pm 1\text{mm}$ ;  $E_w=60\pm 2\text{mm}$  thick)

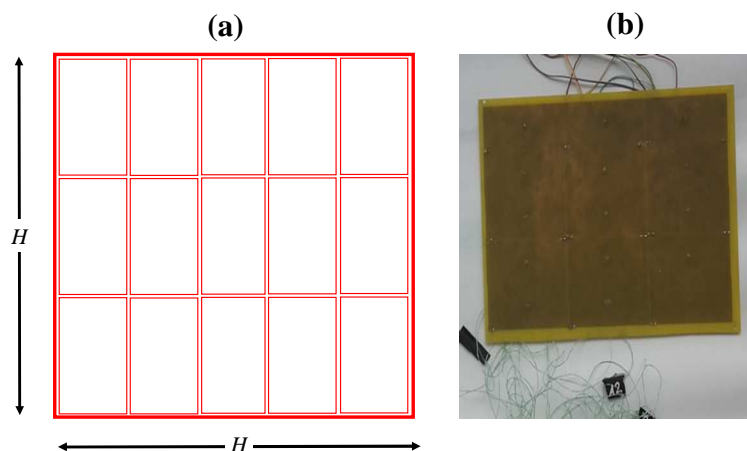


**Fig. 3.** The hot plate (a) schema (b) photography

Electrical wiring and thermocouples emerge from both sides of the wall to avoid possible interference. Electrical resistances have the same values, within  $\pm 2\%$ , in the temperature range considered in this work. The average steady state surface temperature of this wall is denoted as  $\overline{T_h}$ . It is obtained through the arithmetic average of the local temperatures.

Two configurations are treated in this work:

- simple wall (conventional Trombe wall, Fig. 4a);
- wall equipped with vertical and transparent partitions (Fig. 4b) in glass of length  $L_v=0.8L$ , with the same thickness and thermo-optical characteristics as the exterior glass cover. The partitions are vertically arranged between two heating strips and embedded in the wall. The purpose of replacing the large convective cavity by vertical elongated compartmentalized cavities is to modify the overall natural aerodynamics of the assembly and consequently to increase the global natural convective heat transfer. In this configuration, the partitions are remote from the outer glass cover as detailed in the diagram of Fig. 4b.

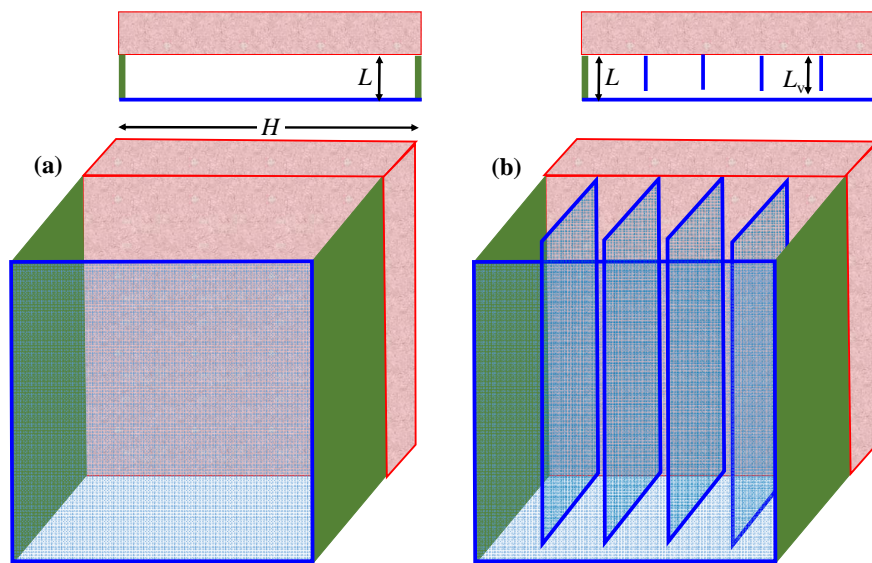


**Fig. 4.** Diagram of the assembly and its profile view  
(a) without partitions (b) with vertical partitions

### 2.3. The active cavity

The natural air flow occurs in the interstitial medium between the hot and cold active walls distant by  $L=55, 110, 165$  and  $220\pm 1$ mm. This distance is adjusted in the present study by sliding the glass into one of the slots provided in the assembly (Fig. 2a). The resulting aspect ratio  $A=L/H$  is of 0.1, 0.2, 0.3 and 0.4. This cavity generating the natural convective flow quantified in the present study constitutes the active part of the assembly.

### 2.4. The passive cavity

When the Trombe wall is in heating mode, the air coming from the active cavity is introduced into a so-called passive cubic cavity, of internal side  $E_{pc}=550\pm 1$ mm. This cavity is thermally insulated on its internal faces with slabs of extruded polyurethane ((3) Fig. 1) of thickness  $E_i=40$ mm and thermal conductivity  $\lambda_p=0.03 \text{ Wm}^{-1}\text{K}^{-1}$  measured with the TPS method. This insulation makes it possible to strongly reduce or even cancel the conductive losses towards the outside environment. It is recalled that the present work does not examine the dynamic operation of the Trombe wall. The exclusive objective of the present study is to quantify the natural convective heat flux occurring in steady state in the active cavity.



Knowledge of this heat flux is essential for the Trombe wall's thermal sizing in a wide range of the Rayleigh number defined as

$$Ra = \frac{g\beta L^4 \rho}{\mu\lambda a} \varphi \quad (1)$$

where  $g$ ,  $\beta$ ,  $\rho$ ,  $\mu$ ,  $\lambda$  and  $a$  are air volumetric expansion coefficient, density, dynamic viscosity, thermal conductivity and thermal diffusivity, while  $g$  is the gravity acceleration and  $\varphi$  the generated heat flux.

### 3. Thermal measurements

Thermal field is measured by means of K type thermocouples of 0.1mm in diameter. After conventional manufacturing through welding, they are systematically calibrated in a thermoregulated bath between 2 and 87°C, by steps of 5°C. A second calibration is done later in situ when all the thermocouples of the assembly are installed in the assembly. This calibration is carried out by arranging the assembly in the climatic chamber and using a calibrating thermometer with an accuracy of  $\pm 0.1^\circ\text{C}$ . Thermocouples of the assembly are connected to a fast data acquisition system ((2) in Fig. 2a) controlled by a computer ((3) in Fig. 2a). Temperature of the glass cover is measured at 5 points distributed on its diagonals. During the measurement, deviations between the 5 temperatures are of about  $0.1^\circ\text{C}$ , since the assembly is installed in the thermoregulated climate chamber. The cold temperature of the assembly  $T_c$  is the arithmetic average value of the local temperatures. Surface thermal state of the passive cavity is also measured at several points: 5 on each of the 6 internal walls and likewise on the other (external) face. They make it possible to confirm that the conductive losses through the walls are negligible. However, the present study does not involve these temperatures since it only concerns the convective exchange in the active cavity.

Wall temperature is measured:

- on each resistance of the heating plate in 3 points distributed on a diagonal, the welds of the thermocouples being stuck on the back face of the plate (on the resin);
- at the surface of the wall (convective flow side) on each of the 5 vertical strips corresponding to the heating resistances: 15 on the central strip (5 by resistance) and 10 on each of the other strips. Thermocouple welds are installed on the surface with great care, because the surface temperatures  $T_h$  are decisive for the data processing leading to quantify convective heat transfer. Surface temperature of the insulating side wall is measured with the same number of thermocouples as on the convective surface. They are used to control the thermal state of the assembly through a thermal balance and also to evaluate the conductive losses through the insulating material.
- in three points on each partition: at its base, its end, and its middle.

For each processed configuration, the considered temperatures are those obtained in steady state when the maximum fluctuation of all temperatures is less than 0.5%. This condition is reached after approximately 2 to 4 hours of testing, depending on the processed configuration. The slowest correspond to the lowest Rayleigh number, the highest aspect ratio and a partitioned active wall.

### 4. Electrical measurements



Hot plate's electrical resistances are measured through a high resolution multimeter-multiplexer ( $3 \times 10^6$  points) incorporated in the data logger. They are identical within  $\pm 2\%$  in a wide temperature range of 0 to  $90^\circ\text{C}$  corresponding to the intended tests. Resistors are independently electrically powered through a multi-channel stabilized power supply ((4) Fig. 2) whose average precision is of  $\pm 0.1\%$ . Current intensity  $I$  and voltage  $U$  that determine the power generated in each resistor  $P = UI$  are measured with a precision of  $\pm 0.1\%$  and  $0.07\%$  respectively. The relative uncertainty corresponding to the generated power is determined by means of the derivative method used in experimental techniques as  $(\Delta P/P = \Delta U/U + \Delta I/I)$ . Its value ranges from 0.2 to 0.4%, according to the values of the considered couple  $(I, U)$ . Measurements are made in real time by means of a second fast data acquisition system. Electrical measurements considered in the subsequent calculations correspond to the thermal steady state.

## 5. Quantification of natural convective heat transfer

Given the geometry of the processed assembly, convective flow in the active cavity is considered two-dimensional. Only the temperatures of the central column are then considered to determine the distribution of the local convective heat exchange coefficient  $h$  and its average value  $\bar{h}$ . A preliminary calculation has been made in order to determine the contribution of radiation in the global heat transfer. This work was performed through the known radiosity method detailed in [20] considering as grey all the internal elements of the enclosure. Their global IR emissivity varies between 0.06 and 0.11 ( $\pm 7\%$ ), measured by means of the conventional vacuum technique method. Thanks to association of the latter with the thermal field obtained for the highest value of the treated Rayleigh number, considering the glass cover as a single isothermal element at temperature  $T_c$ , calculation shows that radiation is negligible, varying between 1 and 3% of the overall heat transfer. The lateral conductive losses are neglected taking into account only the thermal data of the central column. Losses at the back of the wall were evaluated by using the temperatures measured on the inner and outer faces of the insulating board, corresponding as previously for the largest value of the Rayleigh number. The calculation based on the linearized Fourier law associated with the measured thermal conductivity of the insulator shows that the losses by pure conduction through the insulator are very low, varying between 1 and 2% of the global heat flux. Given these results, the heat flux generated by the heating plate is almost completely exchanged by natural convection in the active cavity. The power  $P$  generated in the central column of the wall allows determination of the corresponding heat flux  $\varphi = P/S$  whose maximal uncertainty  $\Delta\varphi/\varphi = \Delta P/P + 2\Delta H/H$  ranges from 0.6 to 1%.

The average natural convective heat transfer coefficient  $\bar{h}$  is determined by means of the heat balance  $\bar{h} = \varphi / (\bar{T}_h - T_c)$  and then the average Nusselt number with

$$\overline{Nu} = \bar{h} L / \lambda_a \quad (2)$$

whose corresponding relative uncertainty  $\Delta \overline{Nu} / \overline{Nu} \sim \Delta\varphi/\varphi + 2 \Delta T / (\bar{T}_h - T_c) + \Delta L / L$  ranges between 1.4 and 2.3%, obtained by neglecting the uncertainty corresponding to air thermal conductivity  $\lambda_a$ . Considering a complementary margin associated with  $\lambda_a$ , the relative uncertainty retained in this work for  $\overline{Nu}$  is rounded to 5%.

## 6. Results for the wall without partitions

The convective heat transfer for the aspect ratio  $A=0.1$  is quantified through evolution of  $\overline{Nu}$  versus  $Ra$  presented in Fig. 5(a), for all the treated values of the generated heat flux. Values of  $\overline{Nu}$  are accompanied by the corresponding uncertainty margin. Evolution is of power type as confirmed by the logarithmic version of Fig. 5b. Values processed with the least squares optimization method lead to the correlation

$$\overline{Nu} = 0.424 Ra^{0.225} \quad (3)$$

associated with a high coefficient of determination of 0.997, valid in the whole  $Ra$  range varying between  $2.81 \times 10^8$  and  $4.14 \times 10^9$ .

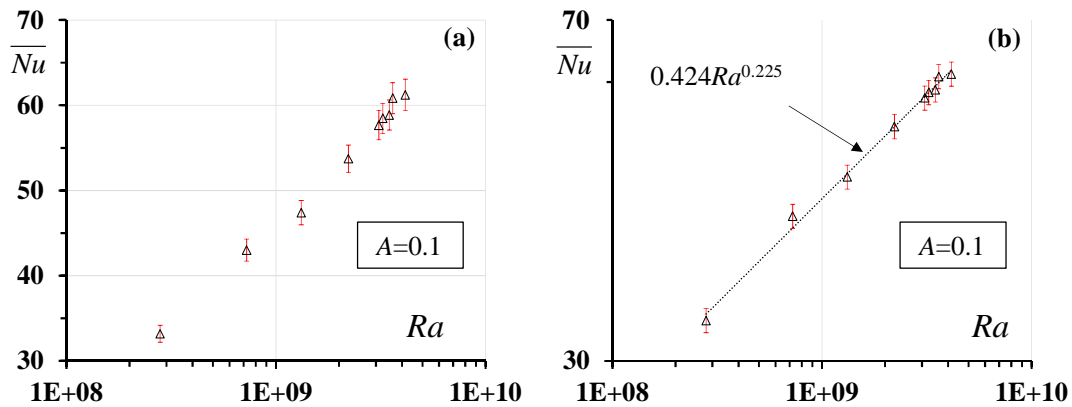


Fig. 5. Evolution of  $\overline{Nu}$  versus  $Ra$  for  $A=0.1$ . Wall without partitions.

Measurements performed for the other treated aspect ratios ( $A = 0.2, 0.3$  and  $0.4$ ) show that the spacing between cavity's active walls improves the average convective transfer in the whole  $Ra$  range, as presented in Fig. 6. Increase of  $\overline{Nu}$  is of about 11.3% when  $A$  increases between 0.1 and 0.2, 13.2% when  $A$  increases between 0.1 and 0.3, and 13.8% when  $A$  increases between 0.1 and 0.4. Their evolutions can be modeled with the power type adjustments shown in Fig. 6a, whose coefficients of determination are respectively of 0.991, 0.992 and 0.996.

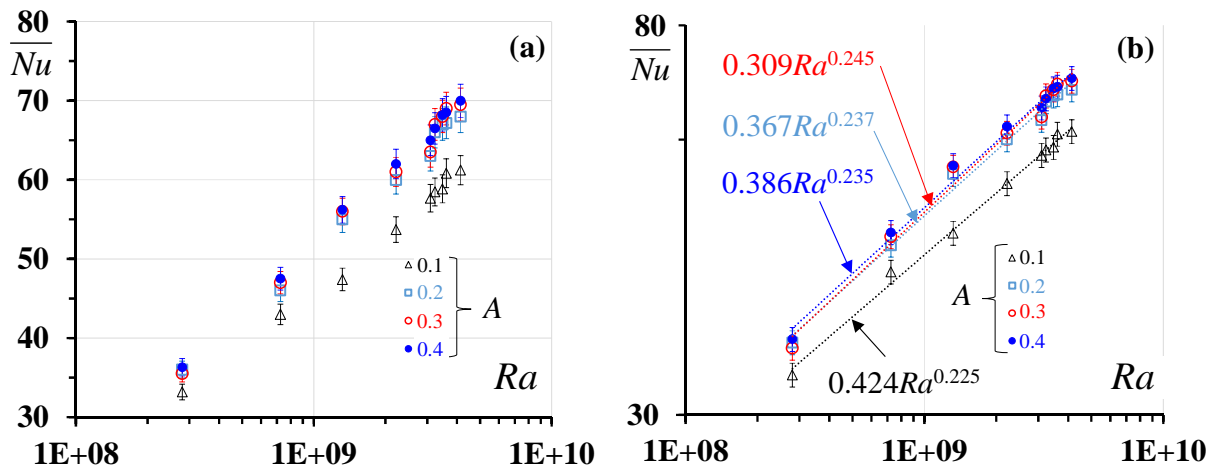
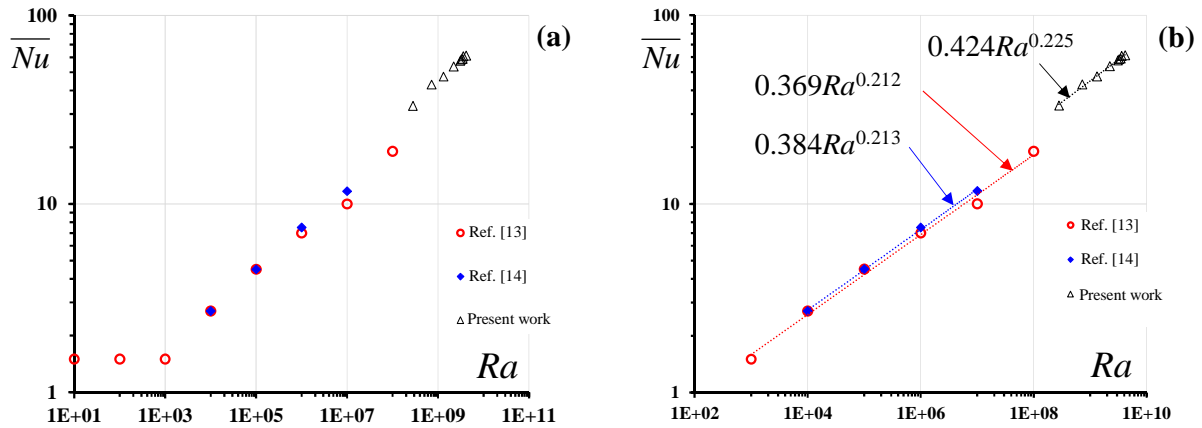


Fig. 6. Influence of  $A$  on  $\overline{Nu}$ . Wall without partitions.

In order to obtain a simple correlation allowing appreciation of the influence of  $A$  on  $\overline{Nu}$ , taking into account the uncertainty margins associated with the measurements, and keeping the original slope (0.225), data processing leads to the following result:

$$\overline{Nu} = (-1.03A^2 + 0.74A + 0.36)Ra^{0.225} \quad (4)$$

Deviation between the values obtained through this correlation (4) and measurements results is low, ranging from -1.7% to 2.5% and therefore included in the experimental error margin. Results of this work have been compared to those of previous studies concerning this low aspect ratio rectangular cavity, dealing with other  $Ra$  ranges. Values presented in Fig. 7a correspond to those of [14], valid for ( $10^4 \leq Ra \leq 10^7$ ;  $A = 1/6$ ) and [13], valid for ( $10^4 \leq Ra \leq 10^8$ ;  $A = 1/7.5$ ). Adjustments presented in Fig. 7b for [14] ( $10^4 \leq Ra \leq 10^7$ ) and [13] ( $10^3 \leq Ra \leq 10^8$ ) are of the power type. They show a coherence between the values obtained for the  $Ra$  ranges corresponding to [13, 14] and those concerning the present study ( $Ra > 2.8 \times 10^8$ ).



**Fig. 7.** Comparison with results of [13] and [14]

Results of [13] also show that for these low cavity aspect ratio:

- $\overline{Nu}$  values are small and close to unity for  $Ra \leq 10^3$ , which is indicative of a stagnant convective flow (pure conductive regime).
- the exponent of  $Ra$  is low, varying between 0.204 and 0.225. This moderate influence of  $A$  was also shown in the study [21], performed with elongated cavities ( $A = 0.75$  and  $1.5$ ) filled with air in the range  $10^4 \leq Ra \leq 10^8$ .

## 7. Results for the wall equipped with partitions

For this configuration, measurements were made under the same conditions as for the previous wall without partitions. Likewise, only thermal and electrical measurements concerning the central band are taken into account. Evolution of the Nusselt number corresponding to the walls without and with partitions, denoted as  $\overline{Nu}$  and  $\overline{Nu}_m$  respectively are presented in Fig. 8(a-d) for  $A = 0.1, 0.2, 0.3$  and  $0.4$  with the corresponding uncertainty bars. These results confirm the effectiveness of the wall equipped with partitions. The aerodynamic phenomena occurring in these elongated cavities systematically increase the average Nusselt number in the whole considered  $Ra$  range for the four considered aspect ratios.

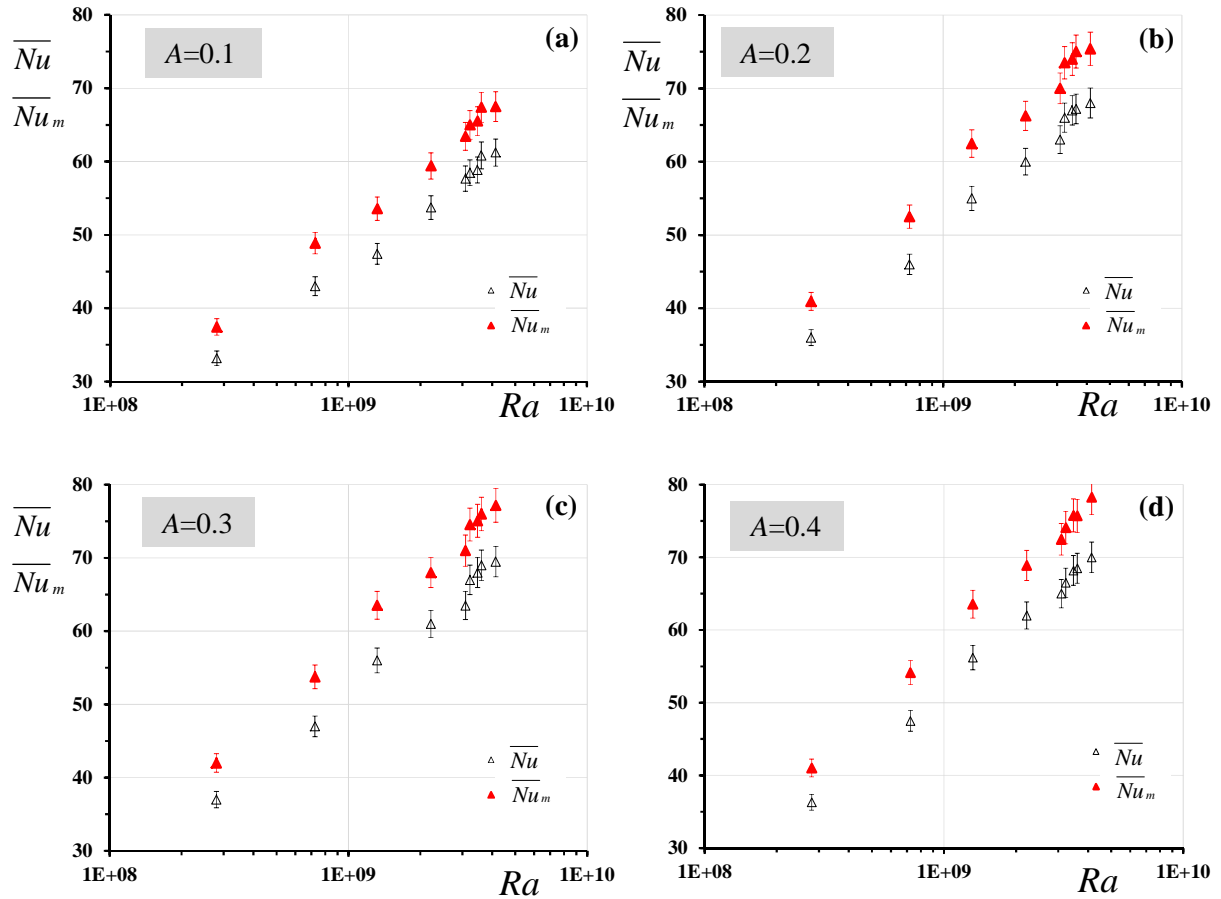


**Fig. 8.** Improvement of the average Nusselt number with interposition of partitions in the wall for  $A=0.1, 0.2, 0.3$  and  $0.4$

The improvement factor

$$r^* = 100(\overline{Nu}_m - \overline{Nu}) / \overline{Nu} \quad (5)$$

presented in Fig. 9 shows an increase of average convective heat transfer between 10.0% and 14.4%, with average values of 11.5%, 11.9%, 11.9% and 12.0% for  $A= 0.1, 0.2, 0.3$  and  $0.4$  respectively. Improvement is more pronounced for the low  $Ra$  values. Taking into account the measurement uncertainty, the average remains relatively maintained for the four considered aspect ratio  $A$ .

In summary, interposition of vertical partitions helps to enhance the natural convective heat transfer in the active cavity of the Trombe wall. For the modified version examined in this work, the corresponding average Nusselt number  $\overline{Nu}_m$  could be determined by means of the correlation

$$\overline{Nu}_m = (1 + r^*) \overline{Nu} \quad (6)$$

being  $\overline{Nu}$  quantified in Eq. (4) while  $r^* = 13.5\%$  and  $10.9\%$  in the  $(2.81 \times 10^8 - 1.32 \times 10^9)$  and  $(2.22 \times 10^9 - 4.14 \times 10^9)$   $Ra$  ranges respectively

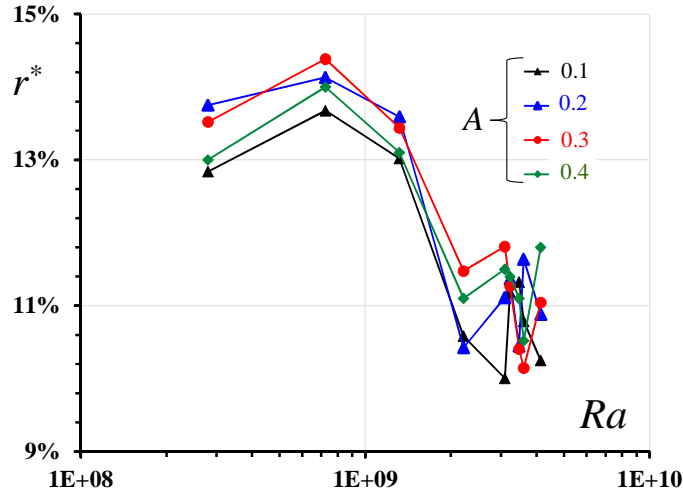


**Fig. 9.** Evolution of the improvement factor  $r^*$  versus  $Ra$  for  $A=0.1, 0.2, 0.3$  and  $0.4$

To make this article easier to read, the values of the main parameters and the measurement uncertainties are summarized in Table 1.

**Table 1** Values of the main considered parameters

	<b>Parameter</b>	<b>Value/ Uncertainty</b>
$A$	aspect ratio	$A=L/H=0.1-0.4$ step 0.1 ( $\pm 0.1\%$ )
$a$	air thermal diffusivity	$2.03 \times 10^{-5} - 2.85 \times 10^{-5} \text{ m}^2 \text{ s}^{-1}$ ( $\pm 3\%$ )
$E$	thickness	$E_v=3.05 \pm 0.02 \text{ mm}$ ; $E_w=60 \pm 1 \text{ mm}$ ; $E_i=40 \text{ mm} \pm 1 \text{ mm}$ ; $E_{pc}=550 \pm 1 \text{ mm}$
$H$	height of the active cavity	$H=550 \text{ mm}$ ( $\pm 1 \text{ mm}$ )
$L$	distance hot-cold walls	$L=AH$ ( $\pm 1 \text{ mm}$ ); $L_v=0.8L$ ( $\pm 1 \text{ mm}$ )
$r^*$	improvement factor	$r^*=10.0\% - 14.4\%$
$Ra$	Rayleigh number	$2.81 \times 10^8 - 4.14 \times 10^9$
$\beta$	air volumetric expansion coefficient	$3.09 \times 10^{-3} - 3.47 \times 10^{-3}$ ( $\pm 1\%$ )
$\Delta m/m$	relative uncertainty	$\Delta U/U=0.1\%$ ; $\Delta I/I=0.07\%$ ; $\Delta P/P=0.2-0.4\%$ ; $\Delta Nu/Nu=5\%$
$\lambda$	thermal conductivity	$\lambda_a=0.021 \text{ W m}^{-1} \text{ K}^{-1}$ ( $\pm 1\%$ ); $\lambda_v=0.95 \pm 0.02 \text{ W m}^{-1} \text{ K}^{-1}$ ( $\pm 1\%$ ); $\lambda_w=1.42 \text{ W m}^{-1} \text{ K}^{-1}$ ( $\pm 1\%$ ); $\lambda_p=0.03 \text{ W m}^{-1} \text{ K}^{-1}$ ( $\pm 1\%$ );
$\mu$	air dynamic viscosity	$1.82 \times 10^{-5} - 2.05 \times 10^{-5} \text{ Pa.s}$ ( $\pm 1\%$ );
$\rho$	air density	$1.028 - 1.204 \text{ kg.m}^{-3}$ ( $\pm 1\%$ )

## 8. Conclusions

This experimental work quantifies the natural convective heat transfer occurring in the active enclosure of a Trombe-type assembly, Results shows that its performance is improved by using a simple device which consists in thin vertical and transparent partitions. Measurements carried out in steady state conditions and controlled thermal environment show that the average natural convective heat transfer can be improved between 10.0% and 14.4%

depending on the aspect ratio of the cavity defined as the ratio between the distance between the active walls and their height. Improvement is also more sensitive for the low Rayleigh number values considered in the tests, which is interesting as they correspond to low solar heat flux values. The study also shows that increase of the aspect ratio between 0.1 and 0.2 enhances the natural convective heat transfer in the active cavity of about 13%. The Nusselt number only slightly increases for higher aspect ratio, in the whole range of the Rayleigh number considered in this work. Measurements are consistent with the results obtained in previous studies for similar cavities and other ranges of the Rayleigh number.

Lastly, correlations are proposed to calculate the average natural convective heat transfer for the Trombe wall without partitions and for its improved version, according to the cavity's Rayleigh number and aspect ratio. Thereby contributing an effective strategy for optimizing the thermal sizing of a Trombe wall's assembly.

## 9. References

- [1] E. Bellos, C. Tzivanidis, E. Zisopoulou, G. Mitsopoulos, K.A. Antonopoulos, An innovative Trombe wall as a passive heating system for a building in Athens—A comparison with the conventional Trombe wall and the insulated wall, *Energy and Buildings* 133 (2016) 754-769.
- [2] F. Stazi, A. Mastrucci, C. di Perna, The behaviour of solar walls in residential buildings with different insulation levels: an experimental and numerical study, *Energy and Buildings* 47 (2012) 217–229.
- [3] G. Gan, A parametric study of Trombe walls for passive cooling of buildings, *Energy and buildings* 27(1) (1998) 37–43.
- [4] Z. Yilmaz, A.B. Kundakci, An approach for energy conscious renovation of residential buildings in Istanbul by Trombe wall system, *Build. Environ.* 43 (2008) 508–517.
- [5] O. Saadatian, K. Sopian, C.H. Lim, Nilofar Asim, M.Y. Sulaiman, Trombe walls: A review of opportunities and challenges in research and development, *Renewable and Sustainable Energy Review* 16 (2012) 6340-6351
- [6] J. Jie, Y. Hua, P. Gang, L. Jianping, Study of PV-Trombe wall installed in a fenestrated room with heat storage, *Applied Thermal Engineering* 27 (2007) 1507–1515.
- [7] E. Krüger, E. Suzuki, A. Matoski, Evaluation of a Trombe wall system in a subtropical location, *Energy and Buildings* 66 (2013) 364–372.
- [8].M. Fahmy, M.M. Mahdy, M. Nikolopoulou, Prediction of future energy consumption reduction using GRC envelope optimization for residential buildings in Egypt, *Energy and Buildings* 70 (2014) 186–193.
- [9] F. Abbassi, N. Dimassi, L. Dehmani, Energetic study of a Trombe wall system under different Tunisian buildig configurations, *Energy and Buildings* 80 (2014) 202-308.
- [10] A. Abdeen, A.A. Serageldin, M.G.E. Ibrahim, A. El-Zafarany, S. Ookawara, R. Murata, Experimental, analytical, and numerical investigation into the feasibility of integrating a passive Trombe wall into a single room, *Applied Thermal Engineering* 154 (2019) 751–768
- [11] C. Balocco, A non-dimensional analysis of a double-faceted energy performance facade, *Energy and Buildings* 36 (2004) 35-40.
- [12] da Silva A.K., Lorente S., A. Bejan, Constructal multi-scale structures for maximal heat transfer density. *Energy* 31 (2006) 620-635.
- [13] S.K.W. Tou, C.P. Tso, X. Zhang, 3-D numerical analysis of natural convective liquid cooling og a 3x3 heater array in rectangular enclosures. *Int. J. Heat Mass Transfer* 42 (1999) 3231-3244.

- [14] C.P. Tso, J.F. Lin, S.K.W. Tou, X.F. Zhang, Flow pattern evolution in natural convection from an array of discrete heat sources in a rectangular cavity at various orientations, *Int. J. Heat Mass Transfer* 47 (2004) 4061-4073.
- [15] A. Purusothaman, A. Bāiri, K. Murugesan, Thermal state of electronic assemblies equipped with an array of heaters and coolers (HACs) subjected to natural convection, *Thermal Science and Engineering Progress* 11 (2019) 317–324.
- [16] A. Bejan, *Convection Heat Transfer*, second ed., Wiley, New York, 1995.
- [17] Hot Disk TPS 2500S <http://www.hotdiskinstruments.com/products/instruments-for-thermal-conductivity-measurements/tps-2500-s.html>
- [18] M. Gustavsson, H. Nagai, T. Okutani, Characterization of anisotropic and irregularly-shaped materials by high-sensitive thermal conductivity measurements. *Solid State Phenomena* 124-126 (2007) 1641-1644.
- [19] Q.C. Wang , Z.C. Wu , X.P. Zhu, The study of the temperature field in an infinite slab under line and plane heat source, *International Journal of Numerical Methods for Heat & Fluid Flow* 25(1) (2015) 25-32.
- [20] A. Bāiri, N. Laraqi, J. M. García de María, Importance of radiative heat exchange in 2D closed diode cavities applied to solar collectors and building, *International Journal of Sustainable Energy* 1 (2005) 33-44.
- [21] A. Bāiri, N. Laraqi, J.M. García de María, Numerical and experimental study of natural convection in tilted parallelepipedic cavities for large Rayleigh numbers, *Experimental Thermal and Fluid Science* 31 (2007) 309-324.